THE JOURNAL OF BIOLOGICAL CHEMISTRY VOL. 291, NO. 35, pp. 18440–18452, August 26, 2016

Integrator of Stress Responses Calmodulin Binding Transcription Activator 1 (Camta1) Regulates miR-212/miR-132 Expression and Insulin Secretion*

Received for publication, January 21, 2016, and in revised form, July 7, 2016 Published, JBC Papers in Press, July 8, 2016, DOI 10.1074/jbc.M116.716860

Inês Guerra Mollet[1], **Helena Anna Malm**, **Anna Wendt**, **Marju Orho-Melander**, and **Lena Eliasson**

From the Department of Clinical Sciences, Clinical Research Centre, Lund University, Jan Waldenströms Gata 35, SE-20502 Malmö, Sweden

Altered microRNA profiles have been demonstrated in experimental models of type 2 diabetes, including in islets of the diabetic Goto-Kakizaki (GK) rat. Our bioinformatic analysis of conserved sequences in promoters of microRNAs, previously observed to be up-regulated in GK rat islets, revealed putative CGCG-core motifs on the promoter of the miR-212/miR-132 cluster, overexpression of which has been shown to increase insulin secretion. These motifs are possible targets of calmodulin binding transcription activators Camta1 and Camta2 that have been recognized as integrators of stress responses. We also identified putative NKE elements, possible targets of NK2 homeobox proteins like the essential islet transcription factor Nkx2-2. As Camtas can function as co-activators with NK2 proteins in other tissues, we explored the role of Camta1, Camta2, and Nkx2-2 in the regulation of the miR-212/miR-132 cluster and insulin secretion. We demonstrate that exposure of control Wistar or GK rat islets to 16.7 mM glucose increases miR-212/miR-132 expression but significantly less so in the GK rat. In addition, Camta1, Camta2, and Nkx2-2 were down-regulated in GK rat islets, and knockdown of Camta1 reduced miR-212/miR-132 promoter activity and miR-212/miR-132 expression, even under cAMP elevation. Knockdown of Camta1 decreased insulin secretion in INS-1 832/13 cells and Wistar rat islets but increased insulin content. Furthermore, knockdown of Camta1 reduced K^+-induced insulin secretion and voltage-dependent Ca^{2+} currents. We also demonstrate Camta1 and Nkx2-2 protein interaction. These results indicate that Camta1 is required not only for expression of the miR-212/miR-132 cluster but at multiple levels for regulating beta cell insulin content and secretion.

CAMTAs[2] are members of a family of calmodulin binding transcription activators that are highly conserved across a wide range of multicellular eukaryotes ranging from *Arabidopsis* through *Drosophila* and *Caenorhabditis* to humans (1–3). CAMTAs were first identified in plants where they are involved in cell differentiation in response to environmental cues (4), and a role for CAMTAs as common integrators to stress responses has been suggested (5). In vertebrates, this protein family appears to consist of only two members, CAMTA1 and CAMTA2.

Recent data have drawn our attention to the possibility of the involvement of CAMTAs in type 2 diabetes (T2D), in particular evidence from genome-wide association studies, which have identified a common genetic variant in *CAMTA1* as associated with T2D (6, 7). Being part of a neuroendocrine tissue, pancreatic islet cells share many functional characteristics with neuronal cells. In this context, it is relevant to point out that several studies have identified involvement of CAMTA1 in neuronal malfunction. A polymorphism in human *CAMTA1* has been associated with neuropsychological test performance (8) and a genetic variation in human *CAMTA1* predisposes individuals to episodic memory performance (9). In neuroblastoma cells, CAMTA1 primarily regulates genes involved in neuronal function and differentiation and is a candidate tumor suppressor (10).

Previous studies have demonstrated that regulation of CAMTAs involves association with class II histone deacetylases (11) and NK2 family proteins. CAMTA2, for example, is activated by dissociation of HDAC5, the activation of which subsequently promotes transcription of genes implicated in cardiac hypertrophy via interaction with an NK2 homeobox transcription factor Nkx2-5 (11, 12). NK2 and related homeobox factors recognize and bind NKE sequence elements with the consensus sequence 5′-NAAGTG-3′ (13). NK2-related proteins are essential regulators of development and differentiation in a variety of organisms and tissues (14–17). Nkx2-2 belongs to this family of homeobox domain-containing proteins; it is a vital transcription factor involved in the development of the ventral vertebrate central nervous system (16), in neuroendocrine differentiation of islet cells in the pancreas (18), and in direct regulation of the insulin gene (19). It is critically involved in establishing mature functional alpha, beta, and PP cells in islets (18), in the maintenance of mature beta cell identity and

* This work was supported by Vetenskapsrådet Project Grant 2012-13147 (to L. E.), Linneus Grant 2006-237 (to Lund University Diabetes Centre), Strategic Research Grant 2009-1039 (to SFO-EXODIAB), Regional Support through ALF-Skåne ALFSKANE-450661, Diabetesfonden Grant DIA 2013-055, and the Albert Påhlsson Foundation. The authors declare that they have no conflicts of interest with the contents of this article.

[1] To whom correspondence should be addressed. Tel.: 46-40-391180; Fax: 46-40-391222; E-mail: inesmollet@gmail.com.

[2] The abbreviations used are: CAMTA, calmodulin binding transcription activator in any organism; Camta, calmodulin binding transcription activator 1 or 2 in rodent; T2D, type 2 diabetes; miRNA, microRNA; Camta1 or CAMTA1, calmodulin binding transcription activator 1 in rodent or human, respectively; Camta2 or CAMTA2, calmodulin binding transcription activator 2 in rodent or human, respectively; Nkx2-2 or NKX2-2, NK2 homeobox 2 in rodent or human, respectively; IBMX, 3-isobutyl-1-methylxanthine; CRE, cAMP-response element; AUC, area under the curve; GK, Goto-Kakizaki; Fsk, forskolin; PLA, proximity ligation assay.

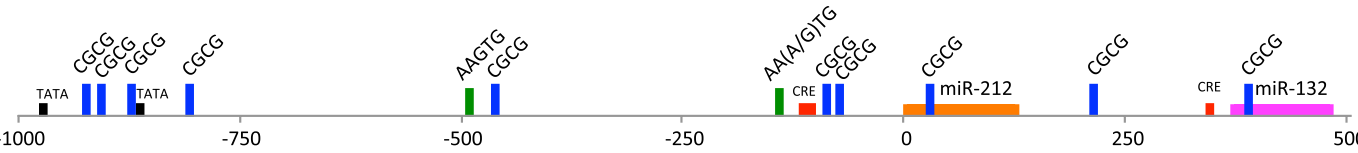

FIGURE 1. **Location of putative CGCG and NKE motifs conserved in human, rat, and mouse and found on the miR-212/miR-132 promoter.** Also represented is the position of two conserved TATA boxes and previously reported CRE (36, 54). Between positions −1000 and −750 bp upstream of the miR-212 hairpin, there are four CGCG motifs, three positioned between two TATA boxes and one just 48 bp downstream of the second TATA box; around −500 bp, there is one CGCG motif 26 bp downstream of the putative NKE element (AAGTG); just upstream of a pair of known CRE sites, there is one additional NKE element, conserved in human and rat, with two additional CGCG motifs 5 and 17 bp downstream of the CRE sites. The start of each microRNA hairpin also harbors a CGCG motif, and an additional motif lies between the two microRNA hairpins.

function (20, 21), and in beta-to-alpha cell reprogramming (22). Additionally, the influence of CAMTAs on neuronal survival has been suggested to be subject to signal-dependent regulation by the MEF2/HDAC5/CaMKII pathway (23), which has recently been targeted as a novel treatment for both type 1 and type 2 diabetes (24).

MicroRNAs (miRNAs) are small non-coding RNAs involved in the regulation of expression of specific target genes at the mRNA level. There is evidence of their involvement in the regulation of insulin secretion and the development of T2D (25). Altered expression of miRNAs has been demonstrated in several experimental models of T2D, including the pancreatic islets of the diabetic Goto-Kakizaki (GK) rat model (26) where 24 microRNAs were found to be up-regulated and six down-regulated when compared with the control Wistar rat (27). However, not much is known regarding the transcriptional regulation of miRNAs. We have previously demonstrated that several of the miRNAs showing altered expression in the GK rat are glucose-dependent (27), and we and others have shown cAMP-dependent regulation of miRNAs (28–30). Specifically, the miR-212/miR-132 cluster has been suggested to be regulated by cAMP through a PKA-dependent mechanism (30) involving cAMP-response element (CRE)-binding proteins and CRTC1 (31).

In this study, we performed a bioinformatic analysis of the promoter of the miR-212/miR-132 cluster, and we identified putative transcription factor binding sites for CAMTAs and NK2 factors. We investigated the possibility of regulation of miR-212/miR-132 expression by CAMTAs and Nkx2-2 in pancreatic islets and clonal beta cells, and we examined effects of CAMTAs on insulin secretion.

Results

Bioinformatic Analysis of miR-212/miR-132 Promoter—To approach the problem of the abnormal miRNA profiles observed in the diabetic GK rat (27), we hypothesized that this might result from disturbed transcriptional regulation of the miRNA genes. To evaluate this, we performed a bioinformatic analysis of the promoters of several up- or down-regulated miRNAs in GK rat islets reported in the literature (27). Using a custom Perl script, we analyzed the frequency of occurrence of DNA sequence motifs, conserved in human, rat, and mouse. This analysis suggested the presence of putative CM2 sequence motifs (A/C/G)CGCG(C/G/T), also called the CG-1 element, on the promoter of the miR-212/miR-132 cluster. This type of motif has been shown to interact with CAMTAs via its N-terminal CG-1 binding domain (5, 32–34). We also identified one putative conserved NKE element 5′-NAAGTG-3′ identical to motifs that bind to NK2-related factors (13) and an additional NK2 element conserved in rats and humans only (Fig. 1).

mRNA Expression of Camta1, Camta2, and Nkx2-2 Is Decreased in GK Rat Islets—To determine whether *Camta1*, *Camta2*, or *Nkx2-2* gene expression might be relevant to diabetes in the GK rat, we investigated mRNA expression of these genes in GK rat islets compared with age-matched control Wistar rat islets. The relative expression of mRNA of the transcription factors was evaluated by real time quantitative reverse transcription PCR after conditioning islets for 24 h in 16.7 mM glucose, to mimic the level of blood glucose observed in the diabetic GK rat model, or for 6 days in 5 mM glucose to expose islets to normal physiological glucose levels for an extended period. In both conditions, we observe a significant reduction of Camta1, Camta2, and Nkx2-2 mRNA expression in GK rat islets compared with Wistar rat islets (Fig. 2, *A*–*C*). This is an indication that bringing glucose to physiological levels for a sustained period in GK islets does not take Camta1, Camta2, or Nkx2-2 mRNA expression to the levels observed in control Wistar rat islets. For Camta1 and Camta2, we did not observe any difference in mRNA expression between the two conditions in the same animal model. However, mRNA expression of Nkx2-2 was significantly increased at 16.7 mM glucose in Wistar islets, and a borderline increase was also observed in GK islets. The increase was significantly less in GK (only 63% increase) than in Wistar islets (2.4-fold increase).

Expression of the miR-212/miR-132 Cluster Is Decreased in GK Rat Islets under Glucotoxicity—After a 6-day incubation of islets in medium at 5 mM glucose, the expression of pri-miR-212/132, miR-212-3p, and miR-132-3p was reduced and identical in diabetic GK and control Wistar rats islets (Fig. 2, *D*–*F*). However, after incubation of islets at 16.7 mM glucose for 24 h, to mimic the blood glucose levels observed in the diabetic GK rat, expression of the primary miRNA transcript, pri-miR-212/132 (Fig. 2*D*), containing both miRNAs and expression of the two 3p mature miRNAs miR-212-3p (Fig. 2*E*) and miR-132-3p (Fig. 2*F*) increased almost 5-fold in the control Wistar rat islets but significantly less so, only 3-fold, in the GK rat islets. Published data on miR-212-3p and miR-132-3p in freshly picked untreated GK islets show that these miRNAs are highly overexpressed when compared with untreated Wistar islets (27). We now show that under glucotoxic conditions in normal Wistar islets the expression of this cluster is even higher than in GK. These data sug-

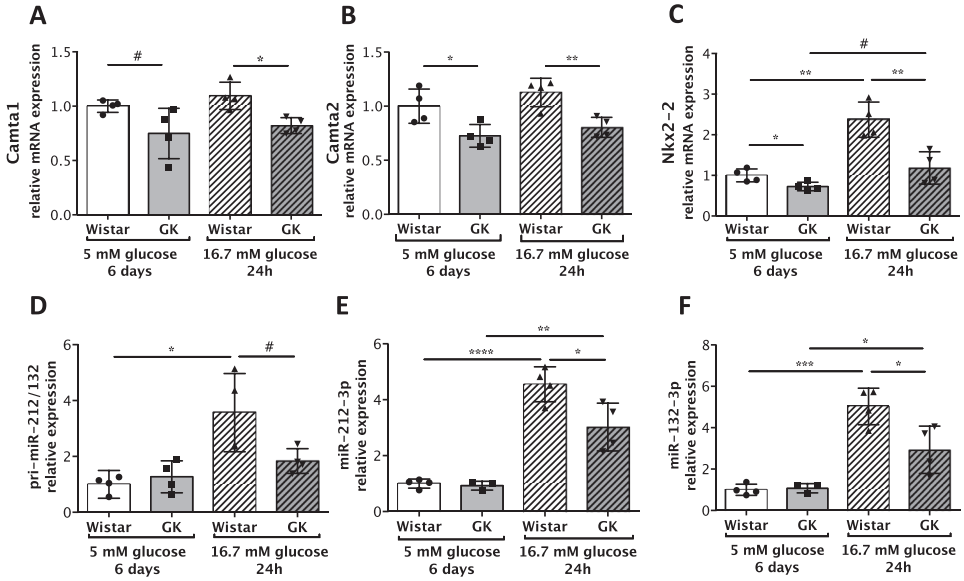

FIGURE 2. **mRNA expression of Camta1, Camta2, Nkx2-2, pri-miR-132, miR-212-3p, and miR-132-3p in diabetic GK rat islets compared with control Wistar islets at 5 mM glucose for 6 days or for 24 h at 16.7 mM glucose.** *A*, Camta1; *B*, Camta2; *C*, Nkx2-2; *D*, pri-miR-132; *E*, miR-212-3p; *F*, miR-132-3p. Data are presented as mean ± S.D.; $n = 4$ animals.

gested that when rat islets are exposed to high glucose levels, Camtas and Nkx2-2 may be necessary for full activation of this miRNA cluster.

Camta1, Camta2, and Nkx2-2 Are Regulated by Glucose in INS-1 832/13 Cells—We next investigated whether Camta1, Camta2, or Nkx2-2 mRNA expression was regulated by glucose in INS-1 832/13 cells. Relative mRNA expression was measured after conditioning cells in medium for 48 h at 2.8, 5, or 16.7 mM glucose. We observed that mRNA expressions of Camta1, Camta2, and Nkx2-2 are all regulated by glucose, with their expression being significantly reduced under glucotoxic conditions in INS-1 832/13 cells (Fig. 3, *A*–*C*), with Camta1 having a 4.6-fold reduction, Nkx2-2 a 3.7-fold reduction, and Camta2 a 2-fold reduction from 2.8 to 16.7 mM glucose. Furthermore, we observed that the expression of the miRNAs miR-212-3p (Fig. 3*D*) and miR-132-3p (Fig. 3*E*) increased concomitantly with increasing glucose concentration, which is in line with our earlier study demonstrating glucose-dependent regulation of miR-212 and miR-132 (27, 31).

miR-212-3p and miR-132-3p Expression Is Decreased after Camta1 Knockdown—We next evaluated expression of miR-212 and miR-132 after knockdown of Camta1, Camta2, or Nkx2-2 in INS-1 832/13 clonal beta-cells and Wistar islets. We verified that in INS-1 832/13 cells the siRNA assay used for Camta1 produced a 90% knockdown of Camta1 mRNA expression, although the scrambled control remained unaffected compared with untreated cells (Fig. 4*A*). On the miRNA level, Camta1 knockdown resulted in a significant decrease in miR-212-3p expression (Fig. 4*B*) and a borderline decrease in miR-132-3p (Fig. 4*C*) when compared with scrambled control. Pri-miR-212/132 expression was also significantly decreased compared with untreated cells (Fig. 4*D*). In Wistar islets, a 32% knockdown of Camta1 was achieved after 72 h (Fig. 4*E*) with a concomitantly significant down-regulation of pri-miR-212/132 expression (Fig. 4*F*). These results suggested that Camta1 might regulate the expression of these miRNAs. Knockdown of Camta2 or Nkx2-2 did not result in significant miR-212-3p of miR-132-3p expression changes in INS-1 832/13 cells (data not shown).

Knockdown of Camta1 Reduces Glucose and High K^+-stimulated Insulin Secretion but Increases Total Insulin—To investigate whether reduced expression of Camtas could affect glucose-stimulated insulin release, insulin secretion was measured in clonal INS-1 832/13 cells after knockdown of Camta1 or Camta2. Knockdown of Camta1 significantly reduced glucose-stimulated insulin secretion at 16.7 mM glucose by 57% (Fig. 5*A*), although a 3–4-fold increase in total insulin content was observed (Fig. 5*B*) under both basal (2.8 mM glucose) and glucose-stimulated (16.7 mM glucose) insulin secretion. Knockdown of Camta2 did not affect glucose-stimulated insulin secretion (data not shown). In Wistar islets, knockdown of Camta1 also significantly reduced insulin secretion (Fig. 5*C*). To see whether Camta1 acts at the final stage of the beta-cell stimulus-secretion coupling, *i.e.* Ca^{2+} influx and/or exocytosis, we circumvented mitochondrial glucose metabolism and the normal cell depolarization by using a high K^+ buffer (50 mM) at 2.8 mM glucose (35); this method causes an artificial cell depolarization by eliminating the K^+ gradient across the membrane. Insulin secretion collected during a 30-min exposure to high K^+ buffer was significantly reduced in INS-1 832/13 cells after knockdown of Camta1 (Fig. 5*D*).

Ca^{2+} Currents Are Reduced by Knockdown of Camta1—To further investigate effects downstream of depolarization, electrophysiological measurements on INS-1 832/13 cells were used to measure differences in exocytosis and voltage-dependent Ca^{2+} currents. Exocytosis was elicited by a train of 10 depolarizing pulses from −70 to 0 mV and was measured as changes in cell membrane capacitance. We observed no difference in the capacitance traces between knockdown and control cells (data not shown). Voltage-dependent Ca^{2+} currents were triggered by membrane depolarizations from a holding potential of −70 mV to membrane potentials ranging from −50 to

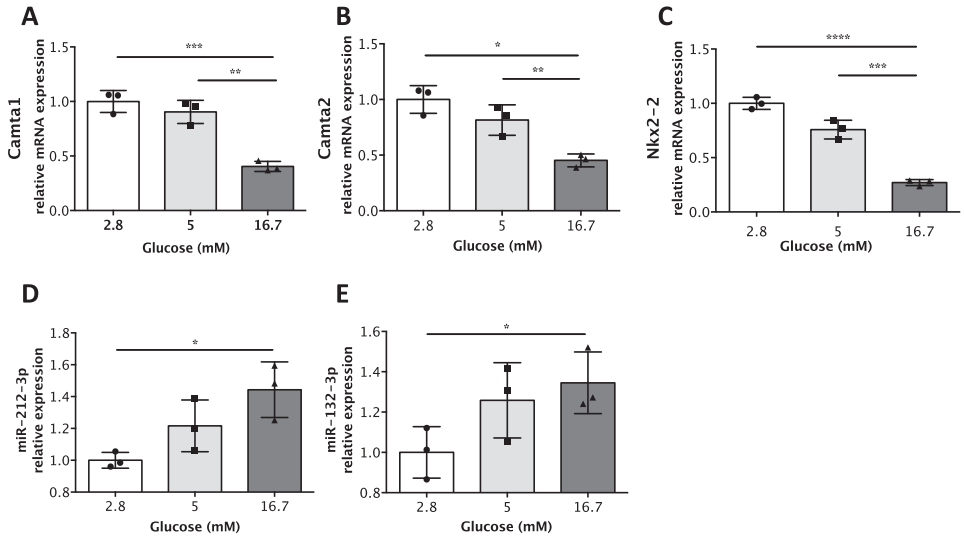

FIGURE 3. **mRNA expression of Camta1, Camta2, Nkx2-2, miR-212-3p, and miR-132-3p in INS-1 832/13 cells after incubation for 48 h in 2.8, 5, or 16.7 mM glucose.** *A*, Camta1; *B*, Camta2; *C*, Nkx2-2; *D*, miR-212-3p; *E*, miR-132-3p. Data are presented as mean ± S.D.; $n = 3$ biological replicates.

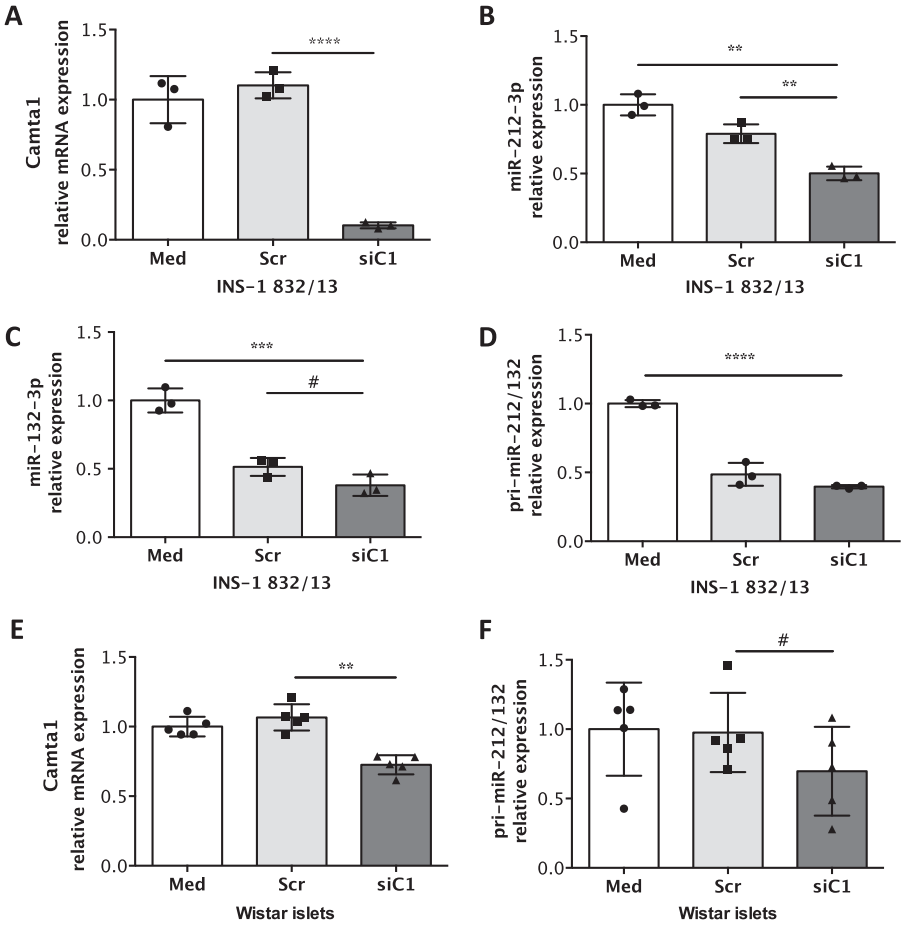

FIGURE 4. **mRNA expression of miR-212-3p and miR-132-3p after knockdown of Camta1.** In INS-1 832/13 cells: *A,* Camta1 knockdown; *B*, miR-212-3p; *C*, miR-132-3p; *D*, pri-miR-212/132. In Wistar rat islets: *E*, Camta1 knockdown; *F*, pri-miR-212/132. Knockdown was performed using siRNA (see "Experimental Procedures"). Untreated medium, *Med*; scrambled negative control, *Scr*; siRNA against Camta1, *siC1*. Data are presented as mean ± S.D.; $n = 3$–5 biological replicates.

+40 mV. At membrane potentials ≥ −10 mV, Ca^{2+} current, measured as charge (Q) passing across the membrane, was significantly reduced by knockdown of Camta1 (Fig. 5, *E* and *F*, AUC as mean ± S.E. and AUC for the IV (Q *versus* V) was as follows: control = $2.5 \times 10^{-10} \pm 3.7 \times 10^{-11}$ and siCamta1 $1.0 \times 10^{-10} \pm 2.4 \times 10^{-11}$, p value = 0.002). Ca^{2+} current (I) was also significantly reduced (AUC for the IV (I_{Ca} *versus* V) was as follows: control $2.9 \times 10^{-9} \pm 4.2 \times 10^{-10}$ and siCamta1 $1.2 \times 10^{-9} \pm 2.8 \times 10^{-10}$, p value = 0.002). No difference was observed in Na^+ current (data not shown).

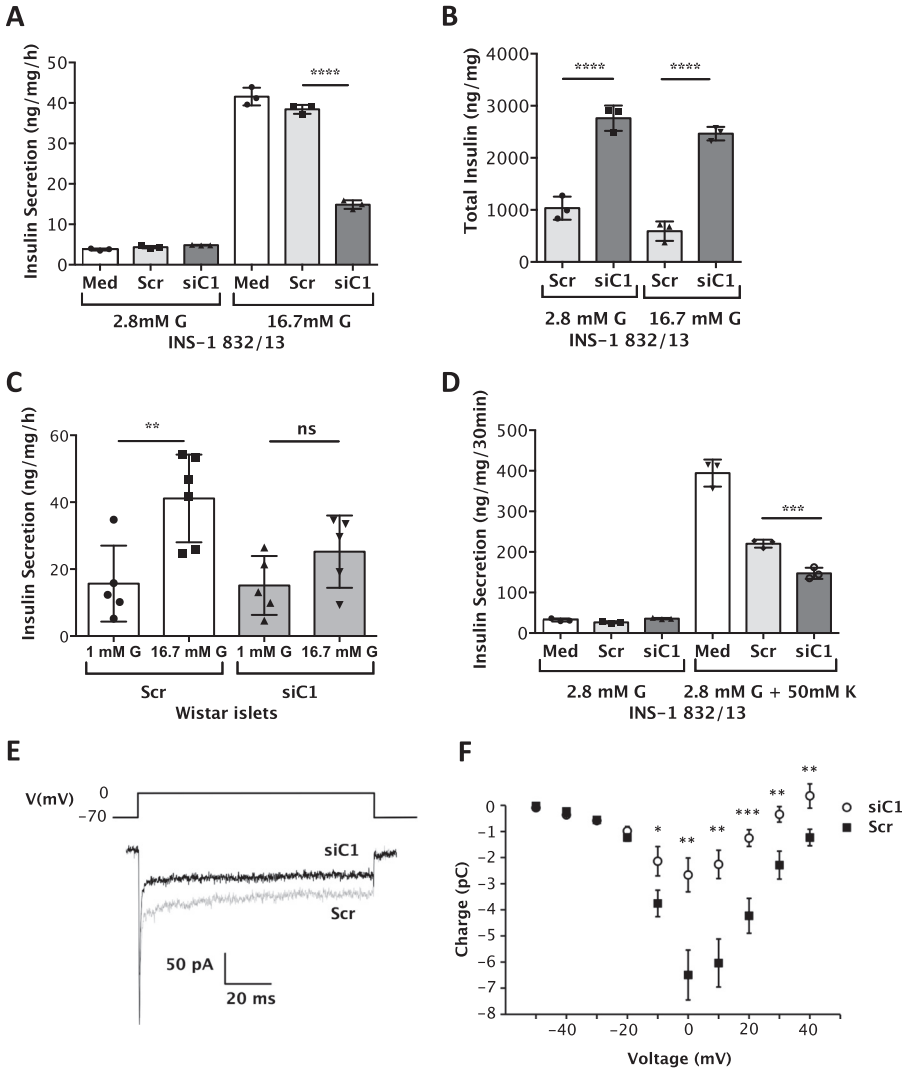

FIGURE 5. **Insulin secretion, total insulin and Ca^{2+} currents after knockdown of Camta1.** Untreated medium, *Med*; scrambled negative control, *Scr*; siRNA against Camta1, *siC1*. Data are presented as mean ± S.D.; $n = 3–6$ biological replicates. In INS-1 832/13 cells: *A*, 1 h of insulin secretion at 2.8 or 16.7 mM glucose (*G*); *B*, total insulin content after 1 h of insulin secretion at 16.7 or 2.8 mM glucose. *C*, 1 h of insulin secretion in Wistar islets at 1 or 16.7 mM glucose; *D*, insulin secretion during a 30-min stimulation with 50 mM K^+ at 2.8 mM glucose in INS-1 832/13 cells; *E* and *F*, recordings of voltage-gated Ca^{2+} channels in single INS-1 832/13 cells: *E*, representative traces of currents evoked by a 100-ms depolarization to 0 mV in a single siC1 cell (*black trace*) and Scr cell (*gray trace*); *F*, charge-voltage relationship measured from single siC1 cells (*white circles*) or Scr cells (*black squares*); the charge is measured as the area enclosed by the curve, starting 12 ms after the onset of the depolarization to exclude the rapidly activating and inactivating Na^+ current. Data are expressed as mean ± S.E. of 22–27 cells.

In Human Islets CAMTA1, CAMTA2, and NKX2-2 mRNA Expression Is Up-regulated by Glucose—In INS-1 832/13 cells, we observed down-regulation of Camta1, Camta2, and Nkx2-2 mRNA expression under glucotoxicity (Fig. 3, *A–C*), and in human islets, we observed instead an up-regulation of CAMTA1, CAMTA2, and NKX2-2 (Fig. 6, *A–C*), although no significant change in hsa-miR-212-3p and hsa-miR-132-3p was observed in the same samples.

Knockdown of Camta1 Decreases Expression of Luciferase from the miR-212/miR-132 Promoter under cAMP Stimulation—To investigate the regulation of the miR-212/miR-132 cluster by Camta1, we cloned a 2.6-kb fragment of the miR-212/miR-132 promoter into a secreted metridia luciferase plasmid pMetLuc2-reporter. After a 6-h incubation in medium containing 16.7 mM glucose or 5 mM glucose with 1 μM forskolin (Fsk) and 10 μM IBMX, we detected increased expression of secreted metridia luciferase (Fig. 7*A*) confirming that, as expected, the cloned miR-212/miR-132 promoter fragment was activated by both high glucose and cyclic AMP stimulation (31, 36). After a 72-h knockdown of Camta1 in INS-1 832/13 cells using siRNA, we transfected the plasmid construct into the cells and observed that after a 6-h incubation at 5 mM glucose with 1 μM forskolin and 10 μM IBMX, activation of metridia luciferase expression was significantly reduced (Fig. 7*B*). No difference in luciferase expression was observed in the same samples after 16 h of incubation at 5 mM glucose (data not shown). After Camta1 knockdown, we also observed a significant down-regulation of pri-miR-212/132 expression by qPCR after a 2-h incubation in Fsk and IBMX (Fig. 7*C*). However, a 2-h incubation in GLP-1 did not significantly alter pri-miR-212/132 expression (Fig. 7*D*).

Camta1 Interacts with Nkx2-2 Differentially at Low and High Glucose and with Respect to Nuclear and Cytoplasmic Localization—Using immunofluorescence confocal microscopy and nuclear co-localization analysis along with a

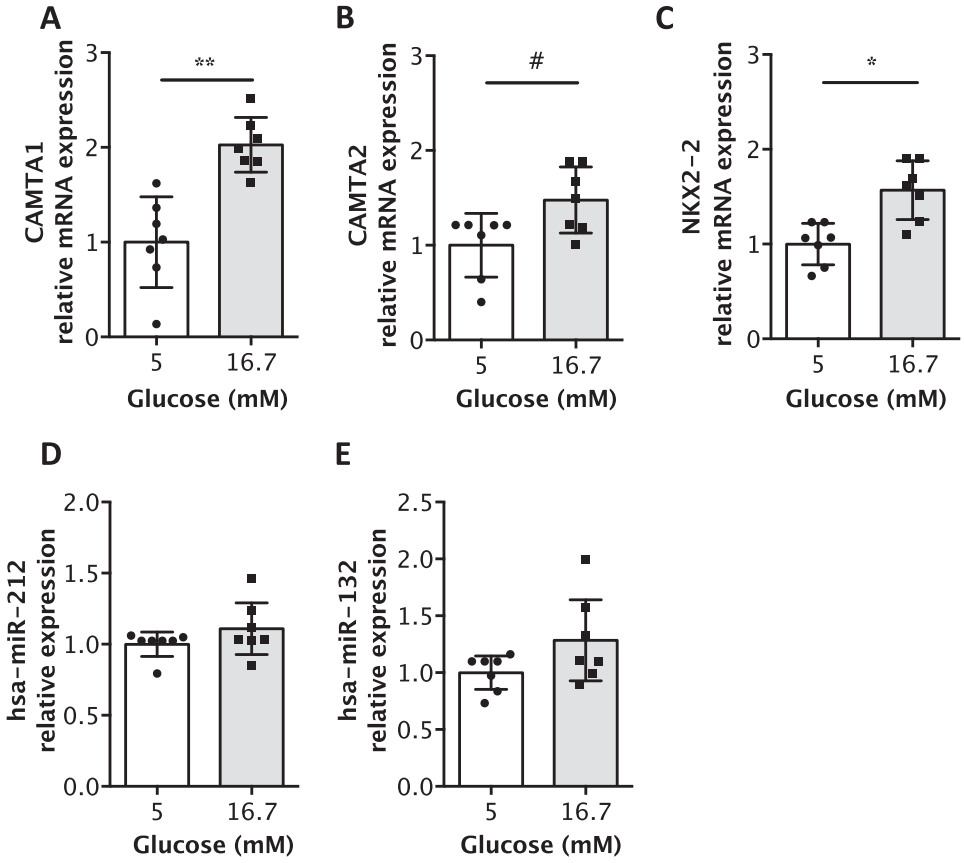

FIGURE 6. **mRNA expression of CAMTA1, CAMTA2, NKX2-2, miR-212-3p, and miR-132-3p in human islets.** Human islets were incubated for 48–62 h at 5 mM or 16.7 mM glucose. *A*, CAMTA1; *B*, CAMTA2; *C*, NKX2-2; *D*, miR-212-3p; *E*, miR-132-3p. Data are presented as mean ± S.D.; $n = 7$ donors.

CAMTA1 antibody that recognizes exon 9 (NBP1-93620, Novus Biologicals), located between the N-terminal CG-1 domain and the downstream TIG domain, we detected Camta1 in both the nucleus and the cytoplasm in INS-1 832/13 cells (Fig. 8*A*). We verified the specificity of the antibody by knockdown of Camta1 with siRNA Silencer Select assay s179516, which targets exons 2 and 3 within the N-terminal CG-1 binding domain. This resulted in decreased Camta1 in both the nucleus and the cytoplasm with an overall reduction of 50% (Fig. 8*B*). To investigate and validate protein interaction between Camta1 and Nkx2-2 in a physiologically relevant context, we performed a proximity ligation assay, which detects protein interactions at less than 40 nm with each fluorescent spot representing a single interaction event. INS-1 832/13 cells were cultured for 48 h in 2.8, 5, or 16.7 mM glucose and subsequently fixed and stained for detection of Camta1 and Nkx2-2 interaction using the Duolink proximity ligation assay. We detected fluorescent signals (Fig. 8, *C* and *D*) at all three glucose concentrations with a significant overall decrease observed both at 2.8 and 16.7 mM glucose compared with 5 mM glucose (Fig. 8*D*). In addition, we observed a significantly lower number of interaction signals in the nucleus at both 2.8 and 16.7 mM glucose, whereas at 5 mM glucose we saw an identical number of interactions in the nucleus and the cytoplasm (Fig. 8*D*).

mRNA Expression of Critical Beta Cell Genes Is Down-regulated after Camta1 Knockdown in INS-1 832/13 Cells—We investigated the effect of knockdown of Camta1 on mRNA expression of Camta2, Nkx2-2, and on known targets of Nkx2-2 central to islet cell function as follows: the islet glucose transporter, *Slc2a2* (also known as *Glut2*), the rat insulin genes 1 and 2 (*Ins1* and *Ins2*), and the transcription factor *MafA*. Knockdown of Camta1 in INS-1 832/13 cells (Fig. 4*A*) produced no effect on Camta2 mRNA expression (Fig. 9*A*). However, Nkx2-2 expression was significantly down-regulated (Fig. 9*B*) as was the expression of Slc2a2, Ins1, Ins2, and MafA (Fig. 9, *C*–*F*).

Discussion

In T2D altered miRNA expression profiles have been observed in human as well as in animal models such as in diabetic GK rat islets, yet the transcriptional regulation of miRNAs has remained largely unexplored. In this study, we present evidence for the involvement of the transcriptional co-activator Camta1 in the regulation of the miR-212/miR-132 cluster, which in turn affects insulin secretion (31). We also show that CAMTAs are expressed in both rodent and human pancreatic islets and that in rat clonal beta cells Camta1 interacts with Nkx2-2 and influences insulin production and secretion via pathways other than miRNA regulation.

Diabetic GK rats present with elevated blood glucose levels ranging from 13 to 22 mM (27). Incubation of GK or Wistar rat islets at 16.7 mM glucose for 24 h, to mimic the effects of high blood glucose observed in the GK rat, resulted in down-regulated mRNA expression of Camta1, Camta2, and Nkx2-2 in GK rat islets compared with Wistar islets. GK and Wistar islets from the same animals were also incubated for 6 days at 5 mM

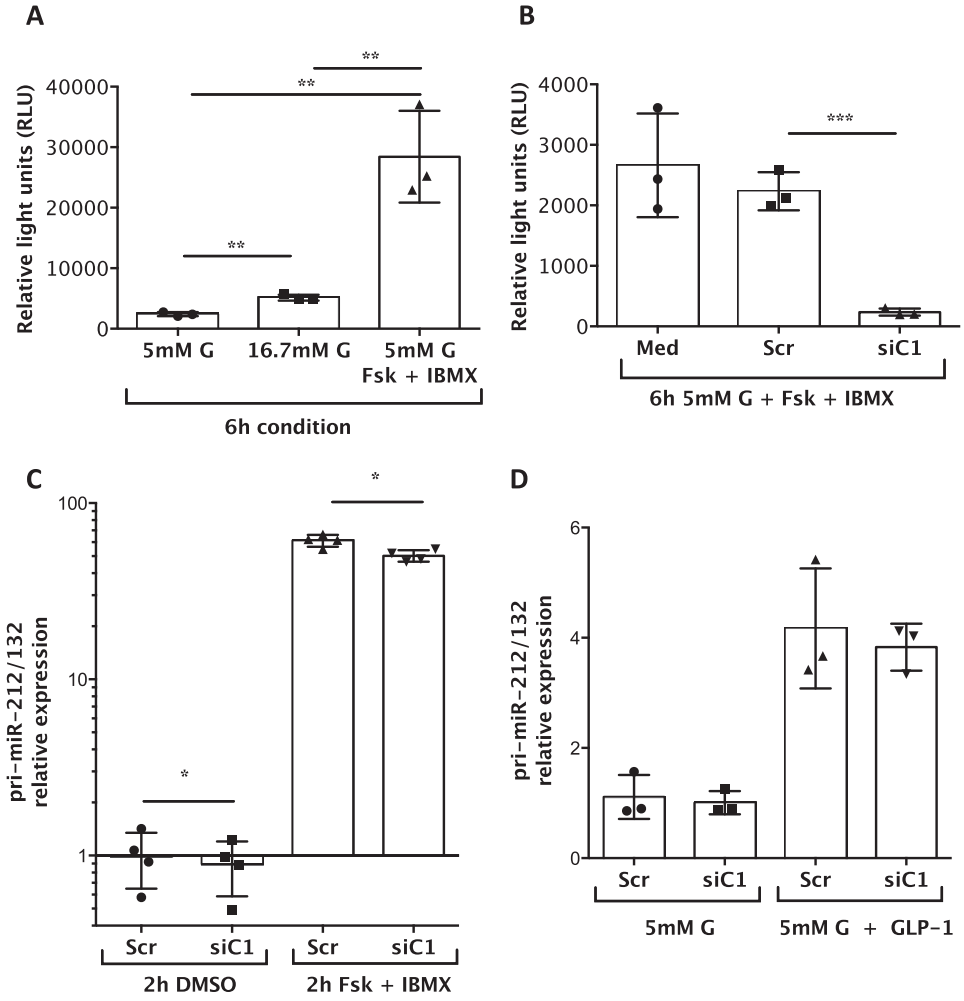

FIGURE 7. **Expression of secreted metridia luciferase from a pMetLuc2-Reporter plasmid under the miR-212/miR-132 promoter after knockdown of Camta1 in INS-1 832/13 cells.** *A*, luciferase expression after a 6-h incubation in 5 mM glucose, 16.7 mM glucose, or under cAMP stimulation with 1 μM Fsk in combination with 10 μM IBMX in 5 mM glucose. *B*, luciferase expression after a 6-h incubation under cAMP stimulation with 1 μM Fsk in combination with 10 μM IBMX in 5 mM glucose following a 72-h knockdown of Camta1. *C*, expression of pri-miR-212/132 under cAMP stimulation with Fsk + IBMX after knockdown of Camta1 (paired Student's *t* test). *D*, expression of pri-miR-212/132 under cAMP stimulation with GLP-1 after knockdown of Camta1. Untreated medium, *Med*; scrambled negative control, *Scr*; siRNA against Camta1, *siC1*. Data are presented as mean ± S.D.; $n = 3–4$ biological replicates.

glucose to see how the expression of these genes in GK rat islets would compare with that of Wistar islets under normal glucose conditions. However, we still observed lower levels of Camta1, Camta2, and Nkx2-2 (Fig. 2) in GK islets under physiological (5 mM) glucose. These data indicate that the down-regulation of these genes may be constitutive in GK rat islets or at least that the down-regulation observed has a relative permanence because it cannot be reversed by incubation of islets at physiological 5 mM glucose for 6 days.

Previous work demonstrated that miR-212 and miR-132 are up-regulated in freshly isolated GK rat islets compared with Wistar islets (27) and that expression of these miRNAs is reduced with increasing glucose concentration in GK islets after 24 h. Here, we confirm and strengthen our previous observation by demonstrating that the up-regulation of both the mature miR-212-3p and miR-132-3p and the pri-miR-212/132 (Fig. 2, *D–F*) in GK islets is significantly diminished after incubation at 16.7 mM glucose for 24 h when compared with the up-regulation observed in control Wistar islets under the same conditions. In contrast, no change was observed in expression of this miRNA cluster after a 6-day incubation at physiological (5 mM) glucose, which suggests that, in contrast to the transcription factors above, expression of these miRNAs is normalized by normoglycemia. Knockdown of Camta1 in INS-1 832/13 cells, followed by transfection of a luciferase construct driven by the miR-212/miR-132 promoter, produced no difference in luciferase expression after a 16-h incubation at 5 mM glucose. However, the observation that cAMP-dependent expression of luciferase from the miR-212/miR-132 promoter was significantly reduced after knockdown of Camta1 (Fig. 7, *B* and *C*), and the close proximity of the putative CG-1-binding sites to known cAMP regulatory elements on the miR-212/miR-132 promoter (Fig. 1), suggests that Camta1 may be required for cAMP-dependent transcriptional regulation of the miR-212/miR-132 cluster. However, after knockdown of Camta1, a 2-h incubation of cells with the incretin GLP-1, which also elevates cAMP, did not alter pri-miR-212/132 expression (Fig. 7*D*). This may be due to differing temporal distribution and amplitude of intracellular cAMP signals selectively regulating downstream events (37). These results

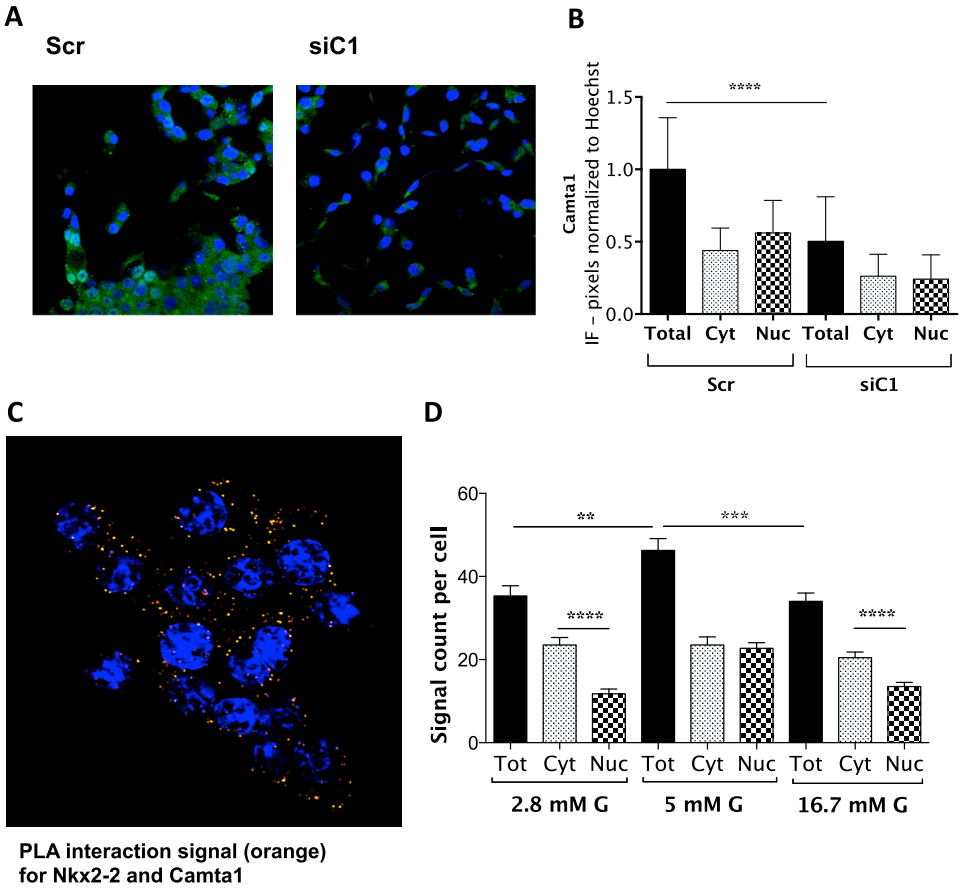

FIGURE 8. **Nuclear and cytoplasmic interaction between Camta1 with Nkx2-2 in INS-1 832/13 cells at 2.8, 5, or 16.7 mM glucose by PLA.** *A*, verification of Camta1 knockdown in the nucleus and cytoplasm by immunofluorescence confocal microscopy in INS-1 832/13 cells; immunofluorescent (*IF*) signal for Camta1 (*green*) and nuclei (*blue*). *B*, quantification of total (*Tot*), nuclear (*Nuc*), and cytoplasmic (*Cyt*) Camta1 knockdown. Cells were treated with siRNA against Camta1 for 72 h. Scrambled negative control, *Scr*; knockdown with siRNA against Camta1, *siC1*. Nuclear co-localization analysis was performed against nuclear stain (Hoechst, *blue*) on non-overlapping images, *n* (*Scr*) = 26 images, and *n* (*siC1*) = 25 images, *n* = 1 biological replicates. *C*, PLA signal in representative cells incubated at 5 mM glucose and stained with antibodies against Camta1 and Nkx2-2 followed by PLA. Nuclei stained with Hoechst. Each PLA signal (*orange*) indicates one detected interaction between Camta1 and Nkx2-2 at less than 40 nM apart. Cells were incubated for 48 h in 2.8, 5, and 16.7 mM glucose (*G*). *D*, quantification of PLA signals performed with Duolink Image Tool (Olink Biosciences). Data are presented as mean ± S.E.; *n* (2.8 mM glucose) = 62 cells; *n* (5 mM glucose) = 76 cells; and *n* (16.7 mM glucose) = 103 cells; *n* = 1 biological replicate.

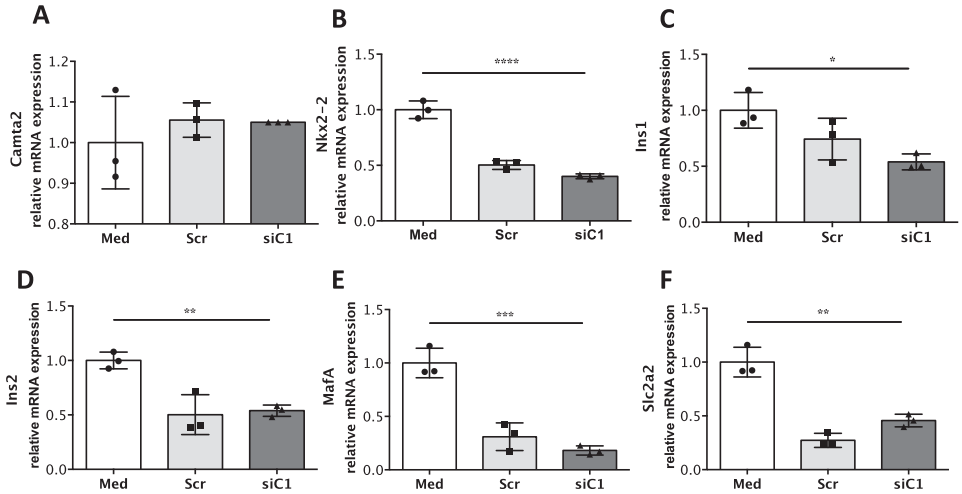

FIGURE 9. **mRNA expression of Camta2, Nkx2-2, Ins1, Ins2, MafA, and Slc2a2 after knockdown of Camta1 in INS-1 832/13 cells.** *A*, Camta2; *B*, Nkx2-2; *C*, Ins1; *D*, Ins2; *E*, MafA; *F*, Slc2a2. Significance was only in relation to untreated control due to interference of the scrambled siRNA control; untreated medium, *Med*; scrambled negative control, *Scr*; siRNA against Camta1, *siC1*. Data are presented as mean ± S.D.; *n* = 3 biological replicates.

are particularly relevant in combination with our recently published observation that the miR-212/miR-132 cluster is regulated by cAMP through de-phosphorylation of CRTC1 and phosphorylation of CREB/ATF1 (31). It would be of interest to further investigate whether Camta1 and CRTC1 act together to regulate the miR-212/miR-132 cluster.

In INS-1 832/13 cells, Camta1 and Camta2 were down-regulated by glucotoxicity (Fig. 3, *A* and *B*). However, in the Wistar rat, we observed no significant change in Camta1 or Camta2 under normoglycemia conditions compared with a 24-h glucotoxic condition (Fig. 2, *A* and *B*), while in human islets both CAMTA1 and CAMTA2 mRNAs were up-regulated under glucotoxic conditions (Fig. 6, *A* and *B*). A recent study revealed differential expression of CAMTA1 in alpha cells compared with beta cells of both human adult and fetal origin, with a 3.7- and 1.8-fold higher expression of CAMTA1 mRNA in fetal and adult alpha cells, respectively (38). In contrast, human islets have been shown to have a greater proportion of alpha cells (39, 40), although in rat islets beta cells are vastly predominant. Although we have not had the opportunity to explore expression of CAMTA1 in response to glucose in alpha and beta cells separately, this may explain the differences in response to glucose observed in INS-1 832/13 clonal beta cells, Wistar rat islets, and human islets, as glucose may induce opposite responses of CAMTA1 expression in alpha and beta cells.

After knockdown of Camta1 in INS-1 832/13 cells and Wistar islets, we observed a significant decrease of glucose-stimulated insulin secretion (Fig. 5, *A* and *C*) but dramatically increased total insulin content (Fig. 5*B*). The decrease in mRNA expression of the rat insulin genes *Ins1* and *Ins2*, both downstream targets of Nkx2-2 (Fig. 9, *C* and *D*), is likely to be a feedback mechanism to down-regulate insulin production in the face of excessive levels of insulin present in the cell.

High K^+ buffer stimulation of beta cells allows evaluation of ATP-independent mechanisms of insulin secretion with preferential activation of fast moving insulin granules at the cell periphery, which are more critically dependent on localized Ca^{2+} pools (41, 42). In contrast, glucose has a stimulatory effect on both fast- and slow-moving insulin granules whether near or distanced from the plasma membrane. In the context of high K^+-induced secretion being dependent on Ca^{2+} ion pools localized at the plasma membrane, the observed reduced Ca^{2+} current through plasma membrane Ca^{2+} channels after Camta1 knockdown is in agreement with the reduced insulin secretion upon high K^+ stimulation. This result suggests that Camta1 may be involved either directly in the regulation of voltage-dependent Ca^{2+} currents through its calcium-calmodulin binding domain (3) or through regulation of genes coding for the voltage-dependent Ca^{2+} channels themselves or associated regulatory factors.

Given the reduced insulin secretion observed after knockdown of Camta1 (Fig. 5, *A*, *C,* and *D*) and the reduced Ca^{2+} current (Fig. 5, *E* and *F*), we expected that the depolarization-induced capacitance increase would have diminished, reflecting reduced exocytosis, in the electrophysiological measurements. However, capacitance traces only tell us that we have electrical contact between a vesicle and the plasma membrane and not how much insulin is actually released. The method used to measure capacitance cannot distinguish between full granule fusion and "kiss-and-run" (or transient granule fusion). The fact that we do not see any difference in depolarization-induced capacitance increase in the context of decreased glucose-induced insulin secretion could be due to increased kiss-and-run transient granule fusion without release of insulin (43). This interpretation could explain the increased insulin content observed (Fig. 5*B*) and indicates that Camta1 may have a direct effect on granule fusion, which warrants further investigation.

Knockdown of Camta1 also decreased expression of Nkx2-2, a transcription factor responsible for establishment of beta cell phenotype and for maintenance of beta cell identity. Knockdown of Nkx2-2 is known to result in reduced insulin secretion and beta cell function (18, 20, 44). In combination with the putative regulatory elements for CAMTAs and NK2 factors identified on the miR-212/miR-132 promoter, these results led us to hypothesize that CAMTA1 and Nkx2-2 might interact to regulate gene expression. CAMTA2, for example, has been implicated in cardiac hypertrophy though interaction with Nkx2-5, an NK2 homeobox transcription factor (11, 12). Indeed, by a proximity ligation assay in rat INS-1 832/13 clonal beta cells, we observed interaction between Camta1 and Nkx2-2. The finding of significantly less interaction in the nucleus, at both 2.8 and 16.7 mM glucose, as opposed to at 5 mM glucose (Fig. 8*D*), suggests that such differential nuclear localization of the interactions occurs as a consequence of abnormal glucose levels, supporting a role for Camta1 in response to physiological stresses. Increase in intracellular Ca^{2+} is intricately linked to the mechanisms that modulate insulin secretion from beta cells (45). In another context, expression of CAMTA1 has been shown to be up-regulated in cells exposed to increased intracellular Ca^{2+}, and this has been associated with novel expression of cardiac transcription factors (46). However, transcription factors can often function as both transcriptional repressors and activators, depending on temporal or cell-specific settings, as is, in fact, the case for Nkx2-2 (19–21, 47, 48).

The knowledge that, in humans, CAMTA1 expression is higher in alpha cells that in beta cells (49) suggests that precisely adequate levels of CAMTA1 may be required to maintain both alpha and beta cell identity in islets along with appropriate expression levels of Nkx2-2. In Fig. 10, we present a summary overview of our results in a rat beta cell. Reduced expression of the glucose transporter Slc2a2 (Glut2) and the islet transcription factor MafA may result from the reduced levels of Nkx2-2 itself after knockdown of Camta1 (Fig. 9). Reduced Slc2a2 expression would contribute to reduced uptake of glucose and thereby to reduced insulin secretion, whereas the reduced expression of MafA, a unique beta cell-specific activator (50) implicated in both insulin biosynthesis and secretion (51), will undoubtedly contribute to the reduced insulin secretion. Our data therefore support the notion that correct levels of Camta1 are crucial at multiple levels, from the detection of glucose, to insulin production and secretion, and beta cell identity. Finally, the normal levels of miR-212 and miR-132 expression obtained in GK rat islets after a 6-day incubation at 5 mM glucose suggest that the requirement for adequate levels of Camta1 may only become evident when blood glucose levels stray beyond normal levels, as is the case in diabetes. This suggests a fundamental role for Camta1 in response to physiological stress. Specifically, our results show that Camta1 is a novel candidate for the regulation of expression of the miR-212/miR-132 cluster. We also show that Camta1 is likely to function alongside Nkx2-2 and

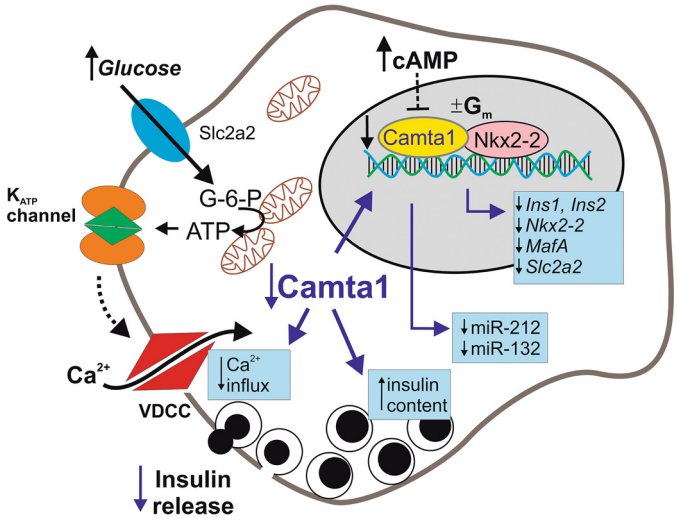

FIGURE 10. **Summary overview of effects of reduced levels of Camta1 at multiple levels in the rat beta cell: reduced insulin secretion; increased insulin content; reduced Ca^{2+} currents; reduced miR-212/miR-132 expression; reduced expression of glucose transporter Slc2a2, insulin genes, Ins1 and Ins2, and beta cell identity transcription factors Nkx2-2, MafA; and a blunted effect on transcription of miR-212/miR-132 under sustained cAMP elevation.** In addition, the molecular interaction between Camta1 and Nkx2-2 in the nucleus is reduced when glucose levels in the medium are either above or below normoglycemia (indicated by $\pm G_m$). Abbreviations used are as follows: *G-6-P*, glucose 6-phosphate; *VDCC*, voltage-dependent calcium channel; K_{ATP} *channel*, ATP-sensitive potassium channel.

cAMP signaling to modulate insulin secretion in the mature islet.

In conclusion, our results provide the first evidence that, in addition to playing a part in the regulation of the miR-212/miR-132 cluster, Camta1 is involved in insulin production and secretion and the pathology of the diabetic GK rat model, suggesting it may play a crucial role in the development of type 2 diabetes.

Experimental Procedures

Materials—All chemicals were purchased from Sigma unless otherwise stated.

Bioinformatic Analysis of miRNA Promoters—Promoter sequence conservation analysis was performed on human, rat, and mouse sequences 1000 bp upstream of the start and 200 bp downstream of the end of selected miRNAs using the Clustalw2 alignment tool (55) and a custom Perl script to determine the frequency of occurrence of short sequence motifs. The analysis was performed on the following microRNAs (27): miR-212/miR-132; miR-375; miR-708; miR-199a-2; miR-199a-1; miR-152; miR-142; miR-130a; miR-124-1; miR-124-2; miR-124-3; miR-7a-1; and miR-7a-2.

Culture of INS-1 832/13 Clonal Cells—The INS-1 832/13 insulin-secreting rat beta-cell line (52) was maintained in RPMI 1640 medium (11.1 mM D-glucose) supplemented with 10% heat-inactivated fetal bovine serum, 100 units/ml penicillin, 100 μg/ml streptomycin, 10 mM HEPES, and 2% (v/v) INS-1 supplement (2 mM L-glutamine, 1 mM sodium pyruvate solution, 50 μM β-mercaptoethanol). All reagents were from HyClone.

Insulin Secretion and Total Insulin—To measure insulin secretion from the INS-1 832/13 cell line, cells were first cultured to confluence in 11.1 mM glucose culture medium in 24-well plates. An overnight incubation in 5 mM glucose medium was performed before the secretion assay. Secretion assay buffer composition (in mM) was as follows: 114 NaCl, 4.7 KCl (68.7 NaCl for 50 KCl secretion), 1.2 KH_2PO_4, 1.16 $MgSO_4$, 20 HEPES, 25.5 $NaHCO_3$, 2.5 $CaCl_2$, and 0.2% bovine serum albumin, pH 7.2. Secretion assays were performed in 4–6 technical replicates. The cells were pre-incubated in 2.8 mM glucose for 30 min followed by 1 h or 30 min conditioning in 2.8 mM glucose (basal secretion), 1 h in 16.7 mM glucose (glucose-stimulated insulin secretion), or 30 min in 2.8 mM glucose with 50 mM KCl secretion buffer (high K^+-stimulated insulin secretion). The secretion buffer was collected from each well, and secreted insulin was determined by radioimmunoassay (Coat-A-Count TKIN2, Siemens) or ELISA (High Range Rat Insulin ELISA, catalog no. 10-1145-01, Mercodia) according to the manufacturers' protocol. Insulin secretion data were normalized to total protein collected from each well using RIPA buffer as described below; total insulin was determined from total protein by ELISA (Mercodia).

Islet Preparations—Rat islets were extracted by collagenase digestion from pancreases of 9–10-week-old male diabetic GK rats (Stockholm colony (53), bred in-house) and age-matched male control Wistar rats (Taconic). Tail blood glucose levels were measured in both GK and Wistar rats before sacrificing the animals in a CO_2 chamber; tail blood glucose ranges were 12–22 mmol/liter (GK) and 4–7 mmol/liter (Wistar). Human islets were obtained through the Human Tissue Lab, Lund University. Islets were hand-picked in Hanks' buffer and incubated in RPMI 1640 medium supplemented with 10% heat-inactivated fetal bovine serum, 100 units/ml penicillin, 100 μg/ml streptomycin, 200 mM glutamine, and the indicated glucose concentration.

RNA Extracts and Relative Gene Expression—All RNA was extracted using miRNeasy kit (Qiagen, catalog no. 217004) with on-column DNase (Qiagen, catalog no. 79254) treatment according to the manufacturer's protocols. RNA concentration was determined using Nanodrop 1000 (Thermo Fisher Scientific). Real time quantitative reverse transcription-PCR was performed using TaqMan assay reagents (Life Technologies, Inc.); cDNA for gene expression was prepared using random primers and High Capacity reverse transcription kit (catalog no. 4368814) on 100 ng of sample RNA; cDNA for miRNA expression was prepared using pooled TaqMan miRNA assay stem loop primers on 10 ng of sample RNA. Relative gene expression was determined using TaqMan Universal PCR Master Mix I (Thermo Fisher) for protein-coding genes and primary miRNA transcript; TaqMan Universal PCR Master Mix II (Thermo Fisher) was used for miRNAs along with TaqMan stem loop primers. Amplification and *Ct* values for three technical replicates of each sample were obtained using ViiA™ 7 real time PCR system and software (Life Technologies, Inc.). Relative gene expression was calculated against expression of two reference genes. The following TaqMan primers were used for rat genes: Camta1 (Rn01051596_m1); Camta2 (Rn01460457_m1); Nkx2-2 (Rn04244749_m1); Ins1 (Rn02121433_g1); Ins2 (Rn01774648_g1); Slc2a2 (Rn00563565_m1); MafA (Rn00845206_s1); and pri-miR-212/132 (Rn03465057_pri), a

69-bp amplicon for primary miRNA transcript containing both miR-212 and miR-132 hairpins and against two reference genes Hprt1 (Rn01527840_m1) and Ppia (Rn00690933_m1). The following TaqMan primers were used for human genes: CAMTA1 (Hs00391998_m1), CAMTA2 (Hs00610789_m1), and NKX2-2 (Hs00159616_m1) against two reference genes HPRT1 (Hs02800695_m1) and B2M (Hs00984230_m1). To detect expression of the mature miRNAs, only the more abundant 3p miRNA sequences were assessed. For rats, the following miRNA TaqMan primers were used: miR-212 (ID 002551) and miR-132 (ID 000457) against two reference small RNAs, U6 snRNA (ID 001973) and U87 (ID 001712). For humans, the following miRNA TaqMan primers were used: miR-212 (ID 000515) and miR-132 (ID 000457) against two reference small RNAs, RNU44 snRNA (ID 001094) and RNU48 (ID 001006).

mRNA Knockdown—mRNA knockdown experiments were performed over 72 h before insulin secretion, plasmid transfection, fixing cells for imaging, or collecting mRNA. The following Silencer® Select pre-designed rat siRNAs (Ambion, Life Technologies, Inc.) were used for mRNA knockdown experiments as follows: (catalog no. 4390771) Camta1 (ID s179516), Camta2 (ID s142512), Nkx2-2 (ID s172641), and Negative Control No. 2 siRNA (catalog no. 4390846)). Transfection was performed using Lipofectamine® RNAiMAX transfection reagent (Life Technologies, Inc., catalog no. 13778150) with complex formation in Opti-MEM® I reduced serum medium (catalog no. 31985-062), and cells were incubated in RPMI 1640 medium as described above with no penicillin or streptomycin added.

Protein Extraction—Total protein was collected by cell lysis with RIPA buffer: 150 mM NaCl, 25 mM Tris-HCl, pH 7.6, 1% Nonidet P-40, 1% sodium deoxycholate, 0.1% SDS. Protein concentration was determined using the Pierce™ BCA protein assay kit (Thermo Scientific).

Plasmid Construct and Luciferase Assay—A 2.6-kb fragment of the promoter region of the miRNA cluster miR-212 and miR-132 was cloned from rat DNA with forward and reverse primers 5′-ATCTCGAGGAGAACCTGCTTCACATCATAGG-3′ and 5′-ATGAATTCACTCCTGATCCCATCAGTTCACCA-3′, respectively. The fragment was inserted into the promoter region of secreted Metridia Luciferase plasmid pMetLuc2-Reporter (Clontech) using GeneArt® seamless cloning and assembly kit (Invitrogen, Life Technologies, Inc.). FuGENE HD transfection reagent (Promega) was used for transfection of the plasmid construct into cells grown in 24-well plates. Secreted Metridia Luciferase expression was evaluated in cell culture medium with Ready-To-Glow™ secreted luciferase reporter assay (Clontech) according to the manufacturer's protocol. Tecan Infinite 200 instrument with Magellan software was used to measure chemiluminescent data in relative light units.

Activation of miR-212/miR-132 Promoter by cAMP—To evaluate robust activation of known cyclic AMP-response elements (CRE) on the promoter of miR-212/miR-132, we stimulated cells with 1 μM forskolin to enhance cAMP production, in combination with 10 μM IBMX, which inhibits cAMP degradation. The incretin GLP-1 at 100 mM was used to evaluate a more physiological but less sustained cytoplasmic cAMP elevation.

Immunostaining and Laser Scanning Confocal Microscopy—For analysis of immunostaining by confocal microscopy, cells were cultured in 8-well chamber slides (Nunc® Lab-Tek® II- CC2™ chamber slide, Sigma) before being fixed with 3% paraformaldehyde, permeabilized with 0.1% Triton X-100, and blocked with 5% normal donkey serum. Immunostaining was performed with rabbit anti-CAMTA1 as primary antibody (NBP1-93620, Novus Biologicals) and donkey DyLight488 anti-rabbit (Jackson 711-485-152) as secondary antibody. Nuclear staining was obtained by incubation in Hoechst (catalog no. 34580, Molecular Probes). Imaging was performed under ×60 magnification with oil immersion on a confocal laser scanning microscope (Zeiss LSM-510) equipped with argon 488 nm and 2-photon lasers. Single or Z-stack images were acquired and analyzed for nuclear co-localization using ZEN 2009 software (Zeiss, Germany).

Proximity Ligation Assay—Protein interaction between Camta1 and Nkx2-2 was evaluated using Duolink (Olink Biosciences) *in situ* proximity ligation assay (PLA). Procedures were followed according to the manufacturer's instructions, using rabbit anti-CAMTA1 (catalog no. NBP1-93620, Novus Biologicals), mouse anti-NKX2.2 (MAB8167, R&D Systems), and Duolink *In Situ* Detection Reagents Orange. Nuclei were stained with Hoechst. Imaging was performed on a laser scanning confocal microscope (Zeiss LSM-510) equipped with a HeNe 543 nm and 2-photon lasers and image acquisition with ZEN 2009 software (Zeiss, Germany). Signal analysis was performed using Duolink Image Tool (Olink Biosciences).

Electrophysiology—Patch pipettes were pulled from borosilicate glass capillaries, coated with sticky wax (Kemdent, UK) and fire-polished to a pipette resistance of 3–6 megohms when filled with the intracellular solution specified below. The standard extracellular solution consisted of (in mM) the following: 118 NaCl, 20 tetraethylammonium chloride (to block voltage-gated K^+ currents), 5.6 KCl, 2.6 $CaCl_2$, 1.2 $MgCl_2$, 5 glucose, and 5 HEPES (pH 7.4 using NaOH). The intracellular solution contained (in mM) the following: ^{125}Cs-glutamate, 10 NaCl, 10 CsCl, 1 $MgCl_2$, 0.05 EGTA, 3 Mg-ATP, 5 HEPES (pH 7.15 using CsOH) and 0.1 cAMP.

The experiments were conducted on single INS-1 832/13 cells 72–96 h after transfection without visualization of the transfected cells. All experiments were performed at 32–34 °C using the standard whole-cell configuration of the patch clamp technique. Changes in membrane capacitance and whole-cell currents were recorded using an EPC-10 patch clamp amplifier and the software PatchMaster (Heka Elektronik, Germany; version 2x90.1). Exocytosis was elicited by a train of 10 depolarizing pulses from −70 to 0 mV applied as 1 Hz. Voltage-dependent Ca^{2+} currents were investigated using an IV protocol where the cell membrane was depolarized from −70 mV to voltages ranging from −50 to + 40 mV for 100 ms. Charge (Q) was measured as the AUC 12 ms after onset of the pulse to exclude the rapidly inactivating Na^+ component.

Statistics—Statistical analyses were performed using GraphPad Prism version 6.00 for Mac (GraphPad Software, La Jolla, CA). Data are presented as mean ± S.D. or ± S.E. as indicated. Statistical significance was evaluated using two-tailed unpaired Student's t test, unless otherwise indicated, with p values indi-

cated as follows: not significant (*ns*) ($p > 0.1$); borderline significance (#) ($0.05 < p < 0.1$); and significant $p < 0.05$ with * ($0.01 < p < 0.05$), ** ($0.001 < p < 0.01$), *** ($0.0001 < p < 0.001$), and **** ($p < 0.0001$).

Author Contributions—I. G. M. conceived the project, conducted most experiments, analyzed and interpreted the results, and wrote the paper. H. A. M. conducted experiments, analyzed data, and revised the manuscript critically. A. W. advised on protocols and design, obtained and analyzed electrophysiological data, and revised the manuscript critically. M. O. M. conceived the project and revised the manuscript critically. L. E. conceived the project, advised on protocols, interpreted the results, and wrote the paper.

Acknowledgments—We thank Britt-Marie Nilsson for pancreas dissection and collagenase islet isolation; Anna-Maria Veljanovska-Ramsay for clonal cell line support; Anna-Maria Dutius Andersson and Enming Zhang for support with confocal imaging; and Olga Göransson for antibody tests and choices. All experimental material obtained from animals was approved by the local ethics committee in Lund/Malmö under Permit M255-12.

References

1. Choi, M. S., Kim, M. C., Yoo, J. H., Moon, B. C., Koo, S. C., Park, B. O., Lee, J. H., Koo, Y. D., Han, H. J., Lee, S. Y., Chung, W. S., Lim, C. O., and Cho, M. J. (2005) Isolation of a calmodulin binding transcription factor from rice (*Oryza sativa* L.). *J. Biol. Chem.* **280,** 40820–40831
2. Bouché, N., Scharlat, A., Snedden, W., Bouchez, D., and Fromm, H. (2002) A novel family of calmodulin binding transcription activators in multicellular organisms. *J. Biol. Chem.* **277,** 21851–21861
3. Finkler, A., Ashery-Padan, R., and Fromm, H. (2007) CAMTAs: calmodulin binding transcription activators from plants to human. *FEBS Lett.* **581,** 3893–3898
4. Eckardt, N. A. (2009) CAMTA proteins: a direct link between calcium signals and cold acclimation? *Plant Cell* **21,** 697
5. Doherty, C. J., Van Buskirk, H. A., Myers, S. J., and Thomashow, M. F. (2009) Roles for *Arabidopsis* CAMTA transcription factors in cold-regulated gene expression and freezing tolerance. *Plant Cell* **21,** 972–984
6. Cauchi, S., Proença, C., Choquet, H., Gaget, S., De Graeve, F., Marre, M., Balkau, B., Tichet, J., Meyre, D., Vaxillaire, M., Froguel, P., and D.E.S.I.R. Study Group. (2008) Analysis of novel risk loci for type 2 diabetes in a general French population: the D.E.S.I.R. study. *J. Mol. Med.* **86,** 341–348
7. Sladek, R., Rocheleau, G., Rung, J., Dina, C., Shen, L., Serre, D., Boutin, P., Vincent, D., Belisle, A., Hadjadj, S., Balkau, B., Heude, B., Charpentier, G., Hudson, T. J., Montpetit, A., *et al.* (2007) A genome-wide association study identifies novel risk loci for type 2 diabetes. *Nature* **445,** 881–885
8. Miller, L. A., Gunstad, J., Spitznagel, M. B., McCaffery, J., McGeary, J., Poppas, A., Paul, R. H., Sweet, L. H., and Cohen, R. A. (2011) CAMTA1 T polymorphism is associated with neuropsychological test performance in older adults with cardiovascular disease. *Psychogeriatrics* **11,** 135–140
9. Huentelman, M. J., Papassotiropoulos, A., Craig, D. W., Hoerndli, F. J., Pearson, J. V., Huynh, K. D., Corneveaux, J., Hänggi, J., Mondadori, C. R., Buchmann, A., Reiman, E. M., Henke, K., de Quervain, D. J., and Stephan, D. A. (2007) Calmodulin binding transcription activator 1 (CAMTA1) alleles predispose human episodic memory performance. *Hum. Mol. Genet.* **16,** 1469–1477
10. Henrich, K. O., Bauer, T., Schulte, J., Ehemann, V., Deubzer, H., Gogolin, S., Muth, D., Fischer, M., Benner, A., König, R., Schwab, M., and Westermann, F. (2011) CAMTA1, a 1p36 tumor suppressor candidate, inhibits growth and activates differentiation programs in neuroblastoma cells. *Cancer Res.* **71,** 3142–3151
11. Song, K., Backs, J., McAnally, J., Qi, X., Gerard, R. D., Richardson, J. A., Hill, J. A., Bassel-Duby, R., and Olson, E. N. (2006) The transcriptional coactivator CAMTA2 stimulates cardiac growth by opposing class II histone deacetylases. *Cell* **125,** 453–466
12. Liu, N., and Olson, E. N. (2006) Coactivator control of cardiovascular growth and remodeling. *Curr. Opin. Cell Biol.* **18,** 715–722
13. Schwartz, R. J., and Olson, E. N. (1999) Building the heart piece by piece: modularity of cis-elements regulating Nkx2-5 transcription. *Development* **126,** 4187–4192
14. Garcia-Fernàndez, J., Baguñà, J., and Saló, E. (1991) Planarian homeobox genes: cloning, sequence analysis, and expression. *Proc. Natl. Acad. Sci. U.S.A.* **88,** 7338–7342
15. Price, M. (1993) Members of the Dlx- and Nkx2-gene families are regionally expressed in the developing forebrain. *J. Neurobiol.* **24,** 1385–1399
16. Price, M., Lazzaro, D., Pohl, T., Mattei, M. G., Rüther, U., Olivo, J. C., Duboule, D., and Di Lauro, R. (1992) Regional expression of the homeobox gene Nkx-2.2 in the developing mammalian forebrain. *Neuron* **8,** 241–255
17. Lints, T. J., Parsons, L. M., Hartley, L., Lyons, I., and Harvey, R. P. (1993) Nkx-2.5: a novel murine homeobox gene expressed in early heart progenitor cells and their myogenic descendants. *Development* **119,** 419–431
18. Sussel, L., Kalamaras, J., Hartigan-O'Connor, D. J., Meneses, J. J., Pedersen, R. A., Rubenstein, J. L., and German, M. S. (1998) Mice lacking the homeodomain transcription factor Nkx2.2 have diabetes due to arrested differentiation of pancreatic beta cells. *Development* **125,** 2213–2221
19. Cissell, M. A., Zhao, L., Sussel, L., Henderson, E., and Stein, R. (2003) Transcription factor occupancy of the insulin gene *in vivo*. Evidence for direct regulation by Nkx2.2. *J. Biol. Chem.* **278,** 751–756
20. Doyle, M. J., and Sussel, L. (2007) Nkx2.2 regulates beta-cell function in the mature islet. *Diabetes* **56,** 1999–2007
21. Doyle, M. J., Loomis, Z. L., and Sussel, L. (2007) Nkx2.2-repressor activity is sufficient to specify alpha-cells and a small number of beta-cells in the pancreatic islet. *Development* **134,** 515–523
22. Papizan, J. B., Singer, R. A., Tschen, S. I., Dhawan, S., Friel, J. M., Hipkens, S. B., Magnuson, M. A., Bhushan, A., and Sussel, L. (2011) Nkx2.2 repressor complex regulates islet beta-cell specification and prevents beta-to-alpha-cell reprogramming. *Genes Dev.* **25,** 2291–2305
23. Long, C., Grueter, C. E., Song, K., Qin, S., Qi, X., Kong, Y. M., Shelton, J. M., Richardson, J. A., Zhang, C. L., Bassel-Duby, R., and Olson, E. N. (2014) Ataxia and Purkinje cell degeneration in mice lacking the CAMTA1 transcription factor. *Proc. Natl. Acad. Sci. U.S.A.* **111,** 11521–11526
24. Christensen, D. P., Dahllöf, M., Lundh, M., Rasmussen, D. N., Nielsen, M. D., Billestrup, N., Grunnet, L. G., and Mandrup-Poulsen, T. (2011) Histone deacetylase (HDAC) inhibition as a novel treatment for diabetes mellitus. *Mol. Med.* **17,** 378–390
25. Esguerra, J. L., Mollet, I. G., Salunkhe, V. A., Wendt, A., and Eliasson, L. (2014) Regulation of pancreatic beta cell stimulus-secretion coupling by microRNAs. *Genes* **5,** 1018–1031
26. Goto, Y., Kakizaki, M., and Masaki, N. (1976) Production of spontaneous diabetic rats by repetition of selective breeding. *Tohoku J. Exp. Med.* **119,** 85–90
27. Esguerra, J. L., Bolmeson, C., Cilio, C. M., and Eliasson, L. (2011) Differential glucose-regulation of microRNAs in pancreatic islets of non-obese type 2 diabetes model Goto-Kakizaki rat. *PLoS ONE* **6,** e18613
28. Jacovetti, C., Abderrahmani, A., Parnaud, G., Jonas, J. C., Peyot, M. L., Cornu, M., Laybutt, R., Meugnier, E., Rome, S., Thorens, B., Prentki, M., Bosco, D., and Regazzi, R. (2012) MicroRNAs contribute to compensatory beta cell expansion during pregnancy and obesity. *J. Clin. Invest.* **122,** 3541–3551
29. Keller, D. M., Clark, E. A., and Goodman, R. H. (2012) Regulation of microRNA-375 by cAMP in pancreatic beta-cells. *Mol. Endocrinol.* **26,** 989–999
30. Shang, J., Li, J., Keller, M. P., Hohmeier, H. E., Wang, Y., Feng, Y., Zhou, H. H., Shen, X., Rabaglia, M., Soni, M., Attie, A. D., Newgard, C. B., Thornberry, N. A., Howard, A. D., and Zhou, Y. P. (2015) Induction of miR-132 and miR-212 expression by glucagon-like peptide 1 (GLP-1) in rodent and human pancreatic beta-cells. *Mol. Endocrinol.* **29,** 1243–1253
31. Malm, H. A., Mollet, I. G., Berggreen, C., Orho-Melander, M., Esguerra, J. L., Göransson, O., and Eliasson, L. (2016) Transcriptional regulation of the miR-212/miR-132 cluster in insulin-secreting beta-cells by cAMP-

regulated transcriptional co-activator 1 and salt-inducible kinases. *Mol. Cell. Endocrinol.* **424,** 23–33
32. Han, J., Gong, P., Reddig, K., Mitra, M., Guo, P., and Li, H. S. (2006) The fly CAMTA transcription factor potentiates deactivation of rhodopsin, a G protein-coupled light receptor. *Cell* **127,** 847–858
33. Yang, T., and Poovaiah, B. W. (2002) A calmodulin binding/CGCG box DNA-binding protein family involved in multiple signaling pathways in plants. *J. Biol. Chem.* **277,** 45049–45058
34. Mitsuda, N., Isono, T., and Sato, M. H. (2003) *Arabidopsis* CAMTA family proteins enhance V-PPase expression in pollen. *Plant Cell Physiol.* **44,** 975–981
35. Olofsson, C. S., Göpel, S. O., Barg, S., Galvanovskis, J., Ma, X., Salehi, A., Rorsman, P., and Eliasson, L. (2002) Fast insulin secretion reflects exocytosis of docked granules in mouse pancreatic B-cells. *Pflugers Arch.* **444,** 43–51
36. Vo, N., Klein, M. E., Varlamova, O., Keller, D. M., Yamamoto, T., Goodman, R. H., and Impey, S. (2005) A cAMP-response element binding protein-induced microRNA regulates neuronal morphogenesis. *Proc. Natl. Acad. Sci. U.S.A.* **102,** 16426–16431
37. Dyachok, O., Isakov, Y., Sågetorp, J., and Tengholm, A. (2006) Oscillations of cyclic AMP in hormone-stimulated insulin-secreting beta-cells. *Nature* **439,** 349–352
38. Blodgett, D. M., Nowosielska, A., Afik, S., Pechhold, S., Cura, A. J., Kennedy, N. J., Kim, S., Kucukural, A., Davis, R. J., Kent, S. C., Greiner, D. L., Garber, M. G., Harlan, D. M., and diIorio, P. (2015) Novel observations from next-generation RNA sequencing of highly purified human adult and fetal islet cell subsets. *Diabetes* **64,** 3172–3181
39. Brissova, M., Fowler, M. J., Nicholson, W. E., Chu, A., Hirshberg, B., Harlan, D. M., and Powers, A. C. (2005) Assessment of human pancreatic islet architecture and composition by laser scanning confocal microscopy. *J. Histochem. Cytochem.* **53,** 1087–1097
40. Cabrera, O., Berman, D. M., Kenyon, N. S., Ricordi, C., Berggren, P. O., and Caicedo, A. (2006) The unique cytoarchitecture of human pancreatic islets has implications for islet cell function. *Proc. Natl. Acad. Sci. U.S.A.* **103,** 2334–2339
41. Hao, M., Li, X., Rizzo, M. A., Rocheleau, J. V., Dawant, B. M., and Piston, D. W. (2005) Regulation of two insulin granule populations within the reserve pool by distinct calcium sources. *J. Cell Sci.* **118,** 5873–5884
42. Eliasson, L., Renström, E., Ding, W. G., Proks, P., and Rorsman, P. (1997) Rapid ATP-dependent priming of secretory granules precedes Ca^{2+}-induced exocytosis in mouse pancreatic B-cells. *J. Physiol.* **503,** 399–412
43. MacDonald, P. E., Braun, M., Galvanovskis, J., and Rorsman, P. (2006) Release of small transmitters through kiss-and-run fusion pores in rat pancreatic beta cells. *Cell Metab.* **4,** 283–290
44. Raum, J. C., Gerrish, K., Artner, I., Henderson, E., Guo, M., Sussel, L., Schisler, J. C., Newgard, C. B., and Stein, R. (2006) FoxA2, Nkx2.2, and PDX-1 regulate islet beta-cell-specific mafA expression through conserved sequences located between base pairs −8118 and −7750 upstream from the transcription start site. *Mol. Cell. Biol.* **26,** 5735–5743
45. Ammälä, C., Eliasson, L., Bokvist, K., Larsson, O., Ashcroft, F. M., and Rorsman, P. (1993) Exocytosis elicited by action potentials and voltage-clamp calcium currents in individual mouse pancreatic B-cells. *J. Physiol.* **472,** 665–688
46. Muller-Borer, B., Esch, G., Aldina, R., Woon, W., Fox, R., Bursac, N., Hiller, S., Maeda, N., Shepherd, N., Jin, J. P., Hutson, M., Anderson, P., Kirby, M. L., and Malouf, N. N. (2012) Calcium-dependent CAMTA1 in adult stem cell commitment to a myocardial lineage. *PLoS ONE* **7,** e38454
47. Watada, H., Mirmira, R. G., Kalamaras, J., and German, M. S. (2000) Intramolecular control of transcriptional activity by the NK2-specific domain in NK-2 homeodomain proteins. *Proc. Natl. Acad. Sci. U.S.A.* **97,** 9443–9448
48. Anderson, K. R., Torres, C. A., Solomon, K., Becker, T. C., Newgard, C. B., Wright, C. V., Hagman, J., and Sussel, L. (2009) Cooperative transcriptional regulation of the essential pancreatic islet gene NeuroD1 (beta2) by Nkx2.2 and neurogenin 3. *J. Biol. Chem.* **284,** 31236–31248
49. Abdel-Aziz, H., Nahrstedt, A., Petereit, F., Windeck, T., Ploch, M., and Verspohl, E. J. (2005) 5-HT3 receptor blocking activity of arylalkanes isolated from the rhizome of Zingiber officinale. *Planta Med.* **71,** 609–616
50. Matsuoka, T. A., Artner, I., Henderson, E., Means, A., Sander, M., and Stein, R. (2004) The MafA transcription factor appears to be responsible for tissue-specific expression of insulin. *Proc. Natl. Acad. Sci. U.S.A.* **101,** 2930–2933
51. Wang, H., Brun, T., Kataoka, K., Sharma, A. J., and Wollheim, C. B. (2007) MAFA controls genes implicated in insulin biosynthesis and secretion. *Diabetologia* **50,** 348–358
52. Hohmeier, H. E., Mulder, H., Chen, G., Henkel-Rieger, R., Prentki, M., and Newgard, C. B. (2000) Isolation of INS-1-derived cell lines with robust ATP-sensitive K^+ channel-dependent and -independent glucose-stimulated insulin secretion. *Diabetes* **49,** 424–430
53. Ostenson, C. G., Khan, A., Abdel-Halim, S. M., Guenifi, A., Suzuki, K., Goto, Y., and Efendic, S. (1993) Abnormal insulin secretion and glucose metabolism in pancreatic islets from the spontaneously diabetic GK rat. *Diabetologia* **36,** 3–8
54. Remenyi, J., Hunter, C. J., Cole, C., Ando, H., Impey, S., Monk, C. E., Martin, K. J., Barton, G. J., Hutvagner, G., and Arthur, J. S. (2010) Regulation of the miR-212/132 locus by MSK1 and CREB in response to neurotrophins. *Biochem. J.* **428,** 281–291
55. McWilliam, H., Li, W., Uludag, M., Squizzato, S., Park, Y. M., Buso, N., Cowley, A. P., and Lopez, R. (2013) Analysis Tool Web Services from the EMBL-EBI. *Nucleic Acids Res.* **41,** W597–W600